

# RELIABILITY ASSESSMENT OF ELECTROMECHANICAL MODULE WITH ASSOCIATION AMONG RELIABILITY INDICATORS

Original scientific paper

UDC:621.833.65:629.017

<https://doi.org/10.46793/aeletters.2024.9.2.3>

Nikolay Petrov<sup>1</sup> , Ventsislav Dimitrov<sup>1\*</sup> , Veselina Dimitrova<sup>1</sup> 

<sup>1</sup>Department MEMETE, FEP of Sliven, Technical University of Sofia, Sliven, 8806, Bulgaria

## Abstract:

This paper presents the reliability assessment results for electromechanical modules, including carbon fiber reinforced composite with thermoplastic matrix, aluminium alloy, and steel housing, through the analysis of competing risks, establishing an association among reliability indicators and non-stationary failure flow using the Weibull probability density function. It has been demonstrated that the estimated probabilities of reliability operations and failure are merely approximations and may deviate from the actual values. This analysis correlates with the estimation of mutual competing risks in the operation of planetary gearbox housing constructed from composite materials. It has been confirmed that the estimated probability of failures is asymptotically effective. A comparative analysis illustrates reliance on simulation methods for planetary gearbox housing made of carbon fiber reinforced composite with a thermoplastic matrix, aluminium alloy, and steel, focusing on parameters such as von Mises stress and deformation (deflection). It has been proven that the electromechanical module, including carbon fiber reinforced composite with thermoplastic matrix, aluminium alloy, and steel planetary gearbox housing is the most reliable, with the lowest heat transfer coefficient, but with the lowest strength.

## ARTICLE HISTORY

Received: 24 March 2024

Revised: 28 May 2024

Accepted: 10 June 2024

Published: 30 June 2024

## KEYWORDS

Carbon fiber reinforced composite, Composite materials, Electromechanical module, Planetary gearbox housing, Reliability, Risk in technical systems (RTS)

## 1. INTRODUCTION

The investigation into the reliability assessment of carbon fiber reinforced composites with a thermoplastic matrix for planetary gearbox housing, as risk technical systems (RTS), is associated with estimating the existence of mutual competing risks and the relationship among reliability indicators and non-stationary failure flow using the Weibull probability density function. In this case, the material consists of polymerisable thermoplastic epoxy resin and high-performance fiber reinforced thermoplastic (FRTP), along with fiber fabrics [1]. The resulting material exhibited good chemical composition and mechanical properties at ambient temperature, with the epoxy resin developed through the direct impregnation

method [2]. The challenge here lies in maintaining the required hardness levels at higher operating temperatures after substituting materials and replacing metals such as aluminium alloy, steel, and magnesium for planetary gearbox housing [3]. For this purpose, the analysis requires the collection of statistical information (data samples). In certain housing, however, this sample is subject to deterministic censorship (incompleteness). The general scenario involving random censorship (incompleteness) extraction is characteristic of RTS. This is provoked by the fact that gearbox housing made from carbon fiber reinforced composites with a thermoplastic matrix, observed during technical usage, could fail due to two or more independent reasons - high temperature and low hardness [4-7]. In other words, although the casing may have

\*CONTACT: Ventsislav Dimitrov, e-mail: [vpdd@abv.bg](mailto:vpdd@abv.bg)

several independent factors leading to failures (competing risks), only one of them is manifested. In this scenario, the presence of an incomplete sample could arise, while the same applies to different types of failures. Therefore, the observed time to failure of an article of  $j^{th}$  kind ( $j=1,..., r$ ) is determined by the realisation of a conventional random quantity (conditioned upon there being no failure of another type) [8,9].

## 2. ASSOCIATION AMONG RELIABILITY INDICATORS

In this paper, an estimation is provided of the probability of planetary gearbox housing serviceability at moment  $t_i$ , to failure within the time interval  $\Delta t = t_i, t_i+1$  due to the  $i^{th}$  housing under the influence of catastrophic functional failure triggered by risks. This probability is referred to as the gross probability [10,11].

The probability of reliability operation ( $P \equiv PRO$ ) is a key quantitative indicator of the elements under investigation [12,13].

Statistically, the probability of reliability operation ( $P$ ) -  $P(t)$  is determined by testing a number of  $N$  elements and monitoring their performance at regular intervals  $\Delta t$ . Faulty components are replaced, and the tests continue until all  $N$  elements have failed [14]. The equation for the probability of reliable operation is:

$$P(t) = \frac{N-n_i}{N}. \quad (1)$$

where is:

-  $n_i$  - is the number of all failed elements/items up to moment  $t_i$ .

As opposed to the event, "reliability operation" is event "failure".

The probabilities for the occurrence of these two events are incompatible and together form a complete group of events, as follows:

$$P(t) + q(t) = 1, \quad (2)$$

therefore:

$$q(t) = 1 - P^*(t) = \frac{n_i}{N}. \quad (3)$$

The function  $q(t)$  represents the probability that the object will fail within a given time interval  $\Delta t$  if it has started at  $t=0$ . The probability of failure  $q(t_1, t_2)$  within the time interval  $(t_1, t_2)$  will be:

$$q(t_1, t_2) = 1 - P(t_1, t_2) = \frac{N(t_1) - N(t_2)}{N(t_1)}. \quad (4)$$

Another indicator of reliability is the density of failure distribution (failure frequency) -  $f(t)$ . The

function  $f(t)$  represents the probability density that the operating time of the object until failure will be less than  $t$ , or in other words, the density of the probability of failure at time  $t$  [15]:

$$f(t) = \frac{\Delta n_i}{N \cdot \Delta t_i}. \quad (5)$$

where is:

-  $\Delta n_i$  - is the number of objects, who failures through the time interval  $\Delta t_i$ .

The failure intensity, denoted as  $\lambda(t)$ , is the conditional density of the probability of failure of the object up to the moment  $t$ , given that there has been no failure of the object until that time.

$$\lambda(t) = \frac{N(t_2) - N(t_1)}{(N - n_i) \cdot \Delta t} = \frac{n(t_2) - n(t_1)}{(N - n_i) \cdot \Delta t}. \quad (6)$$

where are:

-  $N(...)$  - represents the number of operational elements at the relevant moment in time;

-  $n(...)$  - represents the number of failures at the relevant moment in time.

The graphical dependency of  $\lambda(t)$  is illustrated in Fig. 1 and is typical of the planetary gearbox housing made from carbon fiber reinforced composite with a thermoplastic matrix.

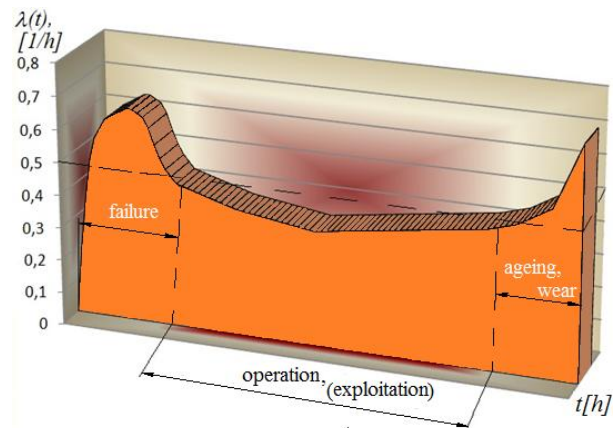


Fig. 1. Graph depicting the change of  $\lambda(t)$  over time

The association among reliability indicators holds practical significance. Often, it is convenient to define indicators in terms of one another, opting for tests with lower costs or greater accuracy in determining unknown parameters. In the exponential distribution law of time for reliable operation  $\lambda(t) = \lambda_0 = const$  (as seen in the period of normal operation in Fig. 1), a characteristic feature is the monotonous increase in failure intensity over time.

Unlike the exponential distribution, where time counting  $t$  begins when the object is determined to

be in a straight state, in the normal distribution, time counting starts from the commencement of the object's operation, i.e., when wearing and ageing processes begin.

The Weibull probability density function for reliable operation is typically employed when the failure flow is non-stationary and the density of the failure flow changes over time [16]:

$$P(t) = e^{-at^k}. \quad (7)$$

$$q(t) = 1 - e^{-at^k}. \quad (8)$$

$$f(t) = akt^{k-1} \cdot p(t). \quad (9)$$

$$\lambda(t) = akt^{k-1} = \frac{f}{T}. \quad (10)$$

$$T = \frac{\frac{1}{k} \cdot f\left(\frac{1}{k}\right)}{\frac{1}{a^k}} = \frac{1}{\lambda_0}. \quad (11)$$

where are:

$a, k$  - parameters of Weibull's distribution law;

$T$  - the time for reliability operation to the first failure;

$f$  - function whose values are given in tabular form.

When  $k=1$ , the Weibull probability density function coincides with the exponential distribution  $\lambda(t)=\lambda_0=const$ . When  $k<1$ , the intensity of failures monotonically decreases; when  $k>1$ , the intensity of failures increases (see Fig. 2).

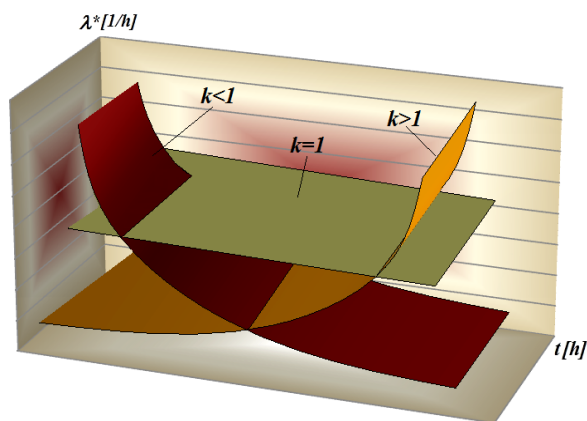


**Fig. 2.** Connection between the Weibull function and the exponential distribution

Another indicator of reliability is the density of failure distribution" with causes that occur in practice, which can be related to the shown equations.

### 3. RELIABILITY ASSESSMENT OF PLANETARY GEARBOX HOUSING INCORPORATING INTO THE ELECTROMECHANICAL MODULE

The system, as depicted in Fig. 3, consists of four parallel connected components: a three-phase asynchronous electric motor with short-circuited rotor, diaphragm coupling, a two-stage planetary gearbox with housing made from, steel, aluminium alloy and carbon fiber reinforced composite with a thermoplastic matrix, flexible rubber tyre coupling combined with multiple disc mechanical torque limiter clutch and welding metal supporting structure.

The motion is transmitted via a joint with the motor shaft to the left semi-coupling (Hub) of the diaphragm coupling. Through driving bolt, gasket and plate pack membrane, the motion is transmitted to right semi-coupling and input shaft of the gearbox. The output shaft of the two-stage planetary gearbox is installed in the hub of the flexible rubber tyre coupling combined with multiple disc mechanical torque limiter clutch.

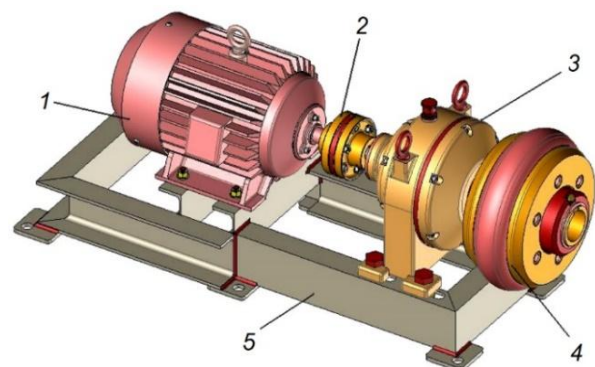


**Fig. 3.** Electromechanical module: 1. Three-phase asynchronous electric motor with short-circuited rotor; 2. Pin and bushing flexible coupling; 3. Two-stage planetary gearbox; 4. Flexible rubber tyre coupling combined with multiple disc mechanical torque limiter clutch; 5. Supporting structure

All elements of the module are mounted on a metal supporting structure, primarily consisting of hot-rolled profiles. Assembly of the individual components of the electromechanical module is conducted through bolt connections [17-20].

Each of the main elements is depicted in the following figures along with its basic components:

- diaphragm coupling – Fig. 4;
- two-stage planetary gearbox – Fig. 5;
- flexible rubber tyre coupling combined with multiple disc mechanical torque limiter clutch – Fig. 6;
- welding metal supporting structure – Fig. 7.

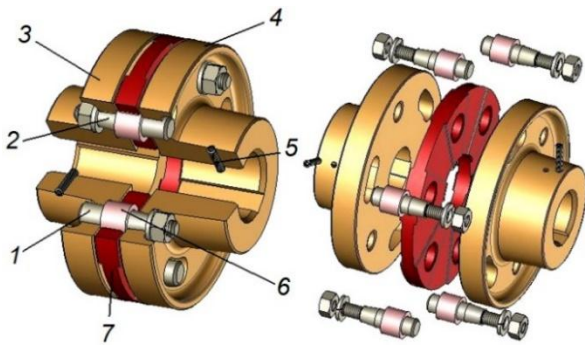


**Fig. 4.** Diaphragm coupling: 1. Driving bolt - right, 2. Driving bolt - left, 3. Left semi-coupling (Hub), 4. Right semi-coupling (Hub), 5. Stop screw, 6. Gasket (collar catch ring), 7. Plate pack membrane (Diaphragm group)

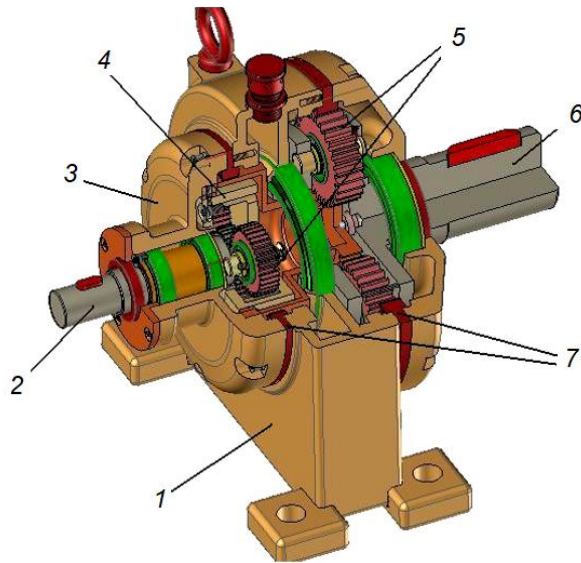


**Fig. 5.** Two-stage planetary gearbox:  
1. Housing, 2. Input shaft, 3. Flange, 4. Planet carrier 1, 5. Planet gear, 6. Output shaft with guide, 7. Ring gear

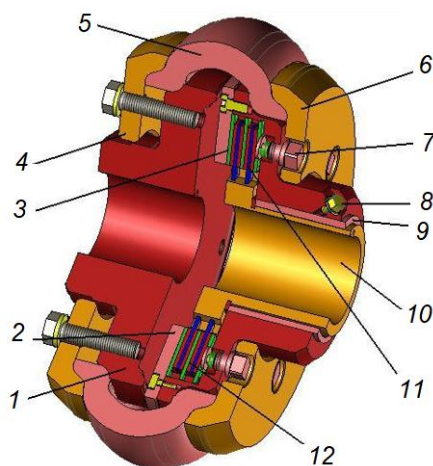


**Fig. 6.** Flexible rubber tyre coupling combined with multiple disc mechanical torque limiter clutch:  
1. Coupling ring - left, 2. Flange, 3. Friction discs, 4,6 – Clamp rings, 5. Rubber tyre flexible elastic element, 7. Fastening bolt, 8. Stop screw, 9. Coupling ring right, 10. Taper bush, 11. Separator discs, 12. Liner

The proposed electromechanical module is structured in such a way that when one of its components fails, the entire system fails:

-the first block failed six times during a period of 960 hours;

-the second one failed 12 times over a period of 1200 hours;

-the third:

- Eight times over a period of 1800 hours (when the gearbox housing is made from steel– I option)

- Six times over a period of 1800 (when the gearbox housing is made from aluminium alloy – II option);

- Five times over a period of 1800 hours (when the gearbox housing is made from carbon fiber reinforced composite with thermoplastic matrices – III option);

-the fourth 18 times over a period of 2700 hours.

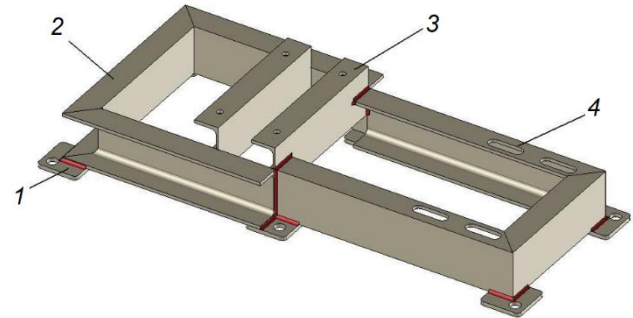


**Fig. 7.** Welding metal supporting structure:  
1. Heel, 2. UPE 120, 3. UPE 100, 4. Alignment holes

To determine the average time for reliable operation of the entire system, given that the exponential law of reliability is valid for each block  $T_0(h)$  [21,22].

Determine the failure intensity of each block using a (Eq.10):

$$\lambda_1 = \frac{6}{960} = 0,006251 \text{ (1/h)}. \quad (12)$$

$$\lambda_2 = \frac{12}{1200} = 0,011 \text{ (1/h)}. \quad (13)$$

$$\lambda_3(I \text{ option}) = \frac{8}{1800} = 0,0044 \text{ (1/h)}. \quad (14)$$

$$\lambda_3(II \text{ option}) = \frac{7}{1800} = 0,0039 \text{ (1/h)}. \quad (15)$$

$$\lambda_3(III \text{ option}) = \frac{5}{1800} = 0,00277 \text{ (1/h)}. \quad (16)$$

$$\lambda_4 = \frac{18}{2700} = 0,00667 \text{ (1/h)}. \quad (17)$$

Determine the intensity of failures of the full system:

$$\lambda_0(I \text{ option}) = \sum_{i=1}^4 \lambda_i = \lambda_1 + \lambda_2 + \lambda_3 + \lambda_4 = 0,02832 \text{ (1/h)}. \quad (18)$$



$$\lambda_0(II \text{ option}) = \sum_{i=1}^4 \lambda_i = \lambda_1 + \lambda_2 + \lambda_3 + \lambda_4 = 0,0278 \text{ (1/h)}. \quad (19)$$

$$\lambda_0(III \text{ option}) = \sum_{i=1}^4 \lambda_i = \lambda_1 + \lambda_2 + \lambda_3 + \lambda_4 = 0,02669 \text{ (1/h)}. \quad (20)$$

Determine the probability of reliable operation for the full system using (Eq.11).

$$T_0(I \text{ option}) = \frac{1}{\lambda_0} = 35,311 \text{ (h)}. \quad (21)$$

$$T_0(II \text{ option}) = \frac{1}{\lambda_0} = 35,97 \text{ (h)}. \quad (22)$$

$$T_0(III \text{ option}) = \frac{1}{\lambda_0} = 37,48 \text{ (h)}. \quad (23)$$

The time for reliable operation until the first failure ( $T$ ) at option I is less compared to option II by 1.87% and option III by 6.1%. The system that includes a two-stage planetary gearbox with a housing made from carbon fiber reinforced composite with a thermoplastic matrix is significantly more reliable.

#### 4. RELIABILITY ASSESSMENT OF PLANETARY GEARBOX HOUSING INCORPORATING INTO THE ELECTROMECHANICAL MODULE

An example involves conducting a comparative analysis using simulation methods of planetary gearbox housing constructed from carbon fiber reinforced composite with a thermoplastic matrix, aluminium alloy, and steel. The analysis focuses on parameters such as stress by von Mises and deformation (deflection). A CAD system, specifically SolidWorks Simulation, is utilised for this purpose.

Petrov et al. [23] and Rachev et al. [24] demonstrate that in determining the efficiency of the estimate  $q(t)$ , it is necessary to find the lower limit of their dispersion.

The following experiment was conducted to determine the probability of recoverability statistically. At moments  $\tau = 0$ , there were  $M$  number of families of failure cases. Their operational capability is restored over time using the same (unchanged) forces and resources. In each time interval  $\Delta\tau_i$ , the number of recovered systems is  $m_i$ .

The law of distribution of the time for detection and correction of failures can be considered exponential. The estimate  $q(t)$  is effective only when the condition in Eg.2 is met, i.e., when only one risk is at play. Under better conditions, the estimate  $q(t)$  is asymptotically effective [25,26].

When using SolidWorks for Finite Element Analysis, the following steps are included [27]:

- create a solid model using the CAD system SolidWorks – Fig. 8a;
- create the Finite Element mesh – Fig. 8b with parameters – Table 1;
- select a material Tables 2, 3 and 4 [14].

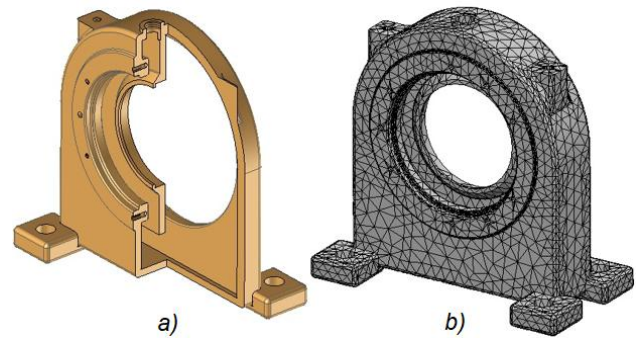


**Fig. 8.** Housing and meshing

a) 3D model of gearbox housing and b) Finite element mesh

**Table 1.** Parameters of finite element mesh

Mesh type	Solid mesh
Mesher used	Current based mesh
Jacobian points	4 point
Max element size	31.1439 mm
Min element size	6.22878 mm
Mesh quality	High
Total nodes	115373
Total elements	69676
Max. aspect ratio	131.12
Percentage of elements with aspect ratio <3	82.7
Percentage of elements with aspect ratio >10	0.396
% of distorted elements	0

**Table 2.** Material properties C22E (1.1151) Steel

EU/EN C22E (1.1151), (AISI 1020 Steel)		
Property	Value	Units
Elastic modules	2e+011	N/m <sup>2</sup>
Poisson's Ratio	0.29	
Shear modulus	7.7e+010	N/m <sup>2</sup>
Mass density	7900	kg/m <sup>3</sup>
Tensile strength	420507000	N/m <sup>2</sup>
Yield strength	351571000	N/m <sup>2</sup>
Thermal expansion coefficient	1.5e-005	1/K
Thermal conductivity	47	W/(mK)
Specific heat	420	J/(kgK)

**Table 3.** Material properties ENAW-3003

Aluminium Alloys ENAW-AlMn1Cu, ENAW-3003		
Property	Value	Units
Elastic modules	6.9e+010	N/m <sup>2</sup>
Poisson's Ratio	0.33	
Shear modulus	2.7e+010	N/m <sup>2</sup>
Mass density	2700	kg/m <sup>3</sup>
Tensile strength	110297000	N/m <sup>2</sup>
Yield strength	41361300	N/m <sup>2</sup>
Thermal expansion coefficient	2.3e-005	1/K
Thermal conductivity	170	W/(mK)
Specific heat	1000	J/(kgK)

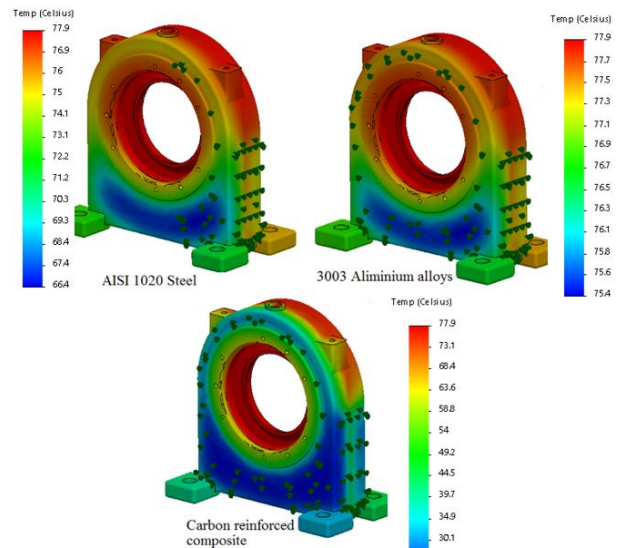
**Table 4.** Carbon fiber reinforced composite with thermoplastic matrix

Carbon fiber reinforced composite with thermoplastic matrix		
Property	Value	Units
Elastic modules	440000000	N/m <sup>2</sup>
Poisson's Ratio	0.35	
Shear modulus	200000000	N/m <sup>2</sup>
Mass density	1497	kg/m <sup>3</sup>
Tensile strength	27579000	N/m <sup>2</sup>
Yield strength	51700000	N/m <sup>2</sup>
Thermal expansion coefficient		1/K
Thermal conductivity	0.23	W/(mK)
Specific heat	1440	J/(kgK)

Structural and thermal simulations are conducted based on thermal verification. Thermal analyses [28] can be performed to determine temperature distribution, temperature gradient, and heat flow within the model.

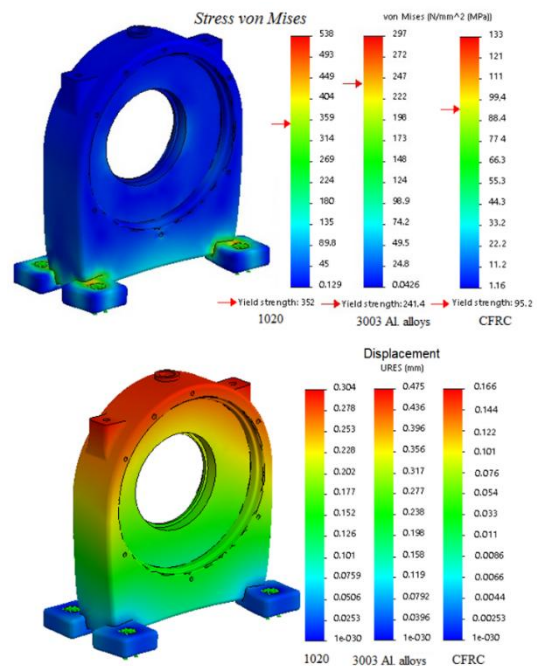
When operating, the maximum temperature reached on the gearbox is  $T=77.9^{\circ}\text{C}$ . A constant convection temperature of  $20^{\circ}\text{C}$  acts on the outer surfaces of the gearbox housing. The results of the thermal analyses are depicted in Fig. 9.

These results indicate that the lowest heat transfer coefficient is observed in the carbon fiber reinforced composite with thermoplastic matrix, while the highest is observed in AISI 1020 steel.

**Fig. 9.** Results of the thermal analyses

To proceed with the analysis:

- Constraints should be created, which are positioned over the holes for the fundamental bolts.
  - Loads should be added, consisting of a combined force with a value of  $F=1450\text{ N}$  and temperatures obtained from the thermal study.
  - Observe the stresses and displacements.
- Results can be viewed as depicted in Fig. 10.

**Fig. 10.** Results of stresses and the displacements

The final stress results indicate that the steel case withstands the highest yield strength, while those from the carbon fiber-reinforced composite with a thermoplastic matrix exhibit the lowest. On the other hand, the composite case shows

displacements three times lower than those observed in aluminium alloys and steel cases.

## 5. CONCLUSION

This paper proposes equations to establish an association among reliability indicators and non-stationary failure flow using the Weibull probability density function.

In connection with this, the following conclusions can be drawn:

- It has been demonstrated that the estimates of reliability operations and probability of failures are merely approximations, deviating from the actual values. This analysis correlates with the estimation of the existence of mutual concurrent risks in the operation of planetary gearbox housing designed from composite materials.

- It has been confirmed that the estimate of the probability of failures is asymptotically effective.

- It has been proven that the time for reliable operation until the first failure for a system which includes a two-stage planetary gearbox with a steel housing is less compared to that for a case made from carbon fiber reinforced composite with thermoplastic matrices by 6.1%.

- An example involves conducting a comparative analysis using simulation methods of planetary gearbox housing constructed from carbon fiber reinforced composite with thermoplastic matrix, aluminium alloy, and steel, focusing on parameters such as von Mises stress and deformation (deflection).

- The results of the thermal analyses indicate that the carbon fiber reinforced composite with a thermoplastic matrix exhibits the lowest heat transfer coefficient, while AISI 1020 steel displays the highest.

- Observing the stresses and displacements reveals that the steel housing withstands the highest yield strength, while the carbon fiber reinforced composite with a thermoplastic matrix exhibits the lowest. Additionally, the composite case has displacements three times lower than those observed in aluminium alloys and steel.

- Observing the stresses and displacements reveals that the steel housing withstands the highest yield strength, while the carbon fiber reinforced composite with a thermoplastic matrix exhibits the lowest. Additionally, the composite case has displacements three times lower than those observed in aluminium alloys and steel.

In future projects, will further explore the dynamics of planetary reducers. Incorporating aspects such as dynamics can contribute to a

deeper understanding of their functionality and applicability. Analogous to the models proposed in [29,30].

## ACKNOWLEDGEMENTS

The authors would like to thank the Research and Development Sector at the Technical University of Sofia for the financial support.

## Conflicts of Interest

The authors declare no conflict of interest.

## REFERENCES

- [1] T. Schneider, M. Kreutzmann, R. Rademacher, C. Dominé, H. Motte, C. Tok, Simulation-driven development of a CFRPT gearbox housing. *The 8<sup>th</sup> International Conference on Computational Methods (ICCM2017)*, 25-29 July 2017, Guilin, Guangxi, China.
- [2] T. Imanishi, H. Nishida, N. Hirayama, N. Tomomitsu, In-situ polymerizable thermoplastic epoxy resin and high performance FRTP using it and fiber fabrics. *16<sup>th</sup> International Conference on Composite Materials*, 8-13 July 2007, Kyoto, Japan, pp.1-6.
- [3] Z. Sun, Y. Dai, H. Hu, C. Guan, G. Tie, X. Chen, Design of Compound Machine Tool for Ultra-Precision Shaft Parts. *MATEC Web of Conferences*, 319, 2020: 01002  
<https://doi.org/10.1051/mateconf/202031901002>
- [4] S. Radojčić, P. Konjatić, M. Katinić, J. Kačmarčik, The Influence of Material Storage on Mechanical Properties and Deterioration of Composite Materials. *Tehnički vjesnik*, 30(5), 2023: 1645-1651.  
<https://doi.org/10.17559/TV-20230308000422>
- [5] I. Demir, M. Ogdu, O. Dogan, S. Demir, Mechanical and physical properties of autoclaved aerated concrete reinforced using carbon fibre of different lengths. *Tehnički vjesnik*, 28(2), 2021: 503-508.  
<https://doi.org/10.17559/TV-20200218194755>
- [6] K.K.H Yeung, K.P. Rao, Mechanical Properties of Kevlar-49 Fibre Reinforced Thermoplastic Composites. *Polymers & Polymer Composites*, 20(5), 2012: 411-424.  
<https://doi.org/10.1177/09673911202000501>

- [7] H.F. Lei, Z.Q. Zhang, B. Liu, Effect of fiber arrangement on mechanical properties of short fiber reinforced composites. *Composites Science and Technology*, 72(4), 2012: 506-514. <https://doi.org/10.1016/j.compscitech.2011.12.011>
- [8] S.M. Letchumanan, T. Arifin, M. Taib, M.Z. Rahim, N.A.N. Salim, Simulating the optimization of carbon fiber reinforced polymer as a wrapping structure on piping system using SolidWorks. *Journal of Failure Analysis and Prevention*, 21, 2021: 2038-2063. <https://doi.org/10.1007/s11668-021-01287-4>
- [9] L. Roblek, K. Gregorin, T. Munih, J. Škofic, Transmission and Hysteresis Error of a Compound Planetary Gearbox. *Svet strojništva*, 12(03/06), 2023. <https://doi.org/10.62020/svet.str.as20230044>
- [10] N. Petrov, V. Dimitrov, V. Dimitrova. Reliability of technology systems in industrial manufacturing. *AkiNik Publications*, New Delhi, India, 2018.
- [11] R. Yankov, Movement of single solid impurities in the boundary layer of a quasi-static two-phase plane current Part I. *International Scientific Conference "UNITECH 2018"*, 16-17 November 2018, Gabrovo, Bulgaria, pp.22-24.
- [12] M. Vasic, B. Stojanovic, M. Blagojevic, Fault analysis of gearboxes in open pit mine. *Applied Engineering Letters*, 5(2), 2020: 50-61. <https://doi.org/10.18485/aeletters.2020.5.2.3>
- [13] S.S. Patil, S. Karuppanan, I. Atanasovska, A.A. Wahab, Contact stress analysis of helical gear pairs, including frictional coefficients. *International Journal of Mechanical Sciences*, 85, 2014: 205-211. <https://doi.org/10.1016/j.ijmecsci.2014.05.013>
- [14] I. Manarikkal, F. Elasha, D. Mba, Diagnostics and prognostics of planetary gearbox using CWT, auto regression (AR) and K-means algorithm. *Applied Acoustics*, 184, 2021: 108314. <https://doi.org/10.1016/j.apacoust.2021.108314>
- [15] P. Zivkovic, M. Milutinovic, M. Tica, S. Trifković, I. Camagi, Reliability Evaluation of Transmission Planetary Gears "bottom-up" approach. *Eksplotacja i Niezawodność - Maintenance and Reliability*, 25(1), 2023: 2. <https://doi.org/10.17531/ein.2023.1.2>
- [16] M. Ognjanović, M. Ristić, P. Živković, Reliability for design of planetary gear drive units. *Meccanica*, 49, 2014: 829-841. <https://doi.org/10.1007/s11012-013-9830-8>
- [17] Z. Daoyong, Z.Li, H. Niaoqing, Multi-Body Dynamics Modeling and Analysis of Planetary Gearbox Combination Failure Based on Digital Twin. *Applied Sciences*, 12(23), 2023: 12290. <https://doi.org/10.3390/app122312290>
- [18] J. Kish, Advanced Rotorcraft Transmission (ART) program status. *27<sup>th</sup> Joint Propulsion Conference*, 24 -26 June 1991, Sacramento, USA. <https://doi.org/10.2514/6.1991-1909>
- [19] H.G. Yoo, W.J. Chung, B.-S. Kim, S.-C. Kim, G.-H. Lee, Application of flexible pin for planetary gear set of wind turbine gearbox. *Scientific Reports*, 12, 2022, 1713. <https://doi.org/10.1038/s41598-022-05828-1>
- [20] M. Stanojević, R. Tomović, L. Ivanović, B. Stojanović, Critical analysis of design of ravigneaux planetary gear trains. *Applied Engineering Letters*, 7(1), 2022: 32-44. <https://doi.org/10.18485/aeletters.2022.7.1.5>
- [21] P. Gao, L. Xie, W. Hu, Reliability and Random Lifetime Models of Planetary Gear Systems. *Shock and Vibration*, 2018, 2018: 9106404. <https://doi.org/10.1155/2018/9106404>
- [22] E. Bai, H. Yang, S. Huang, L. Xie, Reliability modeling of gear system considering strength degradation. *Journal of Physics: Conference Series*, 1885, 2021: 052027. <https://doi.org/10.1088/1742-6596/1885/5/052027>
- [23] N.I. Petrov, K. Y. Dimitrova, D.D. Baskanbayeva, On the reliability of technological innovation systems. *In IOP Conference Series: Materials Science and Engineering*, 1031, 2021: 012044.
- [24] S. Rachev, K. Dimitrova, L. Dimitrov, Study on behaviour of centrifugal pump driven by medium-voltage induction motor during operation control. *E3S Web of Conferences*, 404, 2023: 03005. <https://doi.org/10.1051/e3sconf/202340403005>
- [25] J.E. Akin, Finite Element Analysis Concepts, World Scientific Via SolidWorks. *World Scientific Publishing Co Pte Limited*, New Jersey, USA, 2010. <https://doi.org/10.1142/7785>
- [26] X. Tang, Structural Strength Analysis of Gearbox Casing Based on ABAQUS. *IOP Conference Series: Materials Science and Engineering*, 677, 2019: 052067. <https://doi.org/10.1088/1757-899X/677/5/052067>



- [27] F. Concli, A. Kolios, Preliminary Evaluation of the Influence of Surface and Tooth Root Damage on the Stress and Strain State of a Planetary Gearbox: An Innovative Hybrid Numerical–Analytical Approach for Further Development of Structural Health Monitoring Models. *Computation*, 9(3), 2021: 38.  
<https://doi.org/10.3390/computation9030038>
- [28] Y.F. Cui, Y.H. Zhang, W.D. He, L.J. Dong, Temperature Prediction for 3 MW Wind-Turbine Gearbox Based on Thermal Network Model. *Machines*, 12(3), 2024: 175.  
<https://doi.org/10.3390/machines12030175>
- [29] M. Matejic, M. Blagojevic, M. Matejic, Dynamic behaviour of a planetary reducer with double planet gears. *Mechanical Sciences*, 12(2), 2021: 997-1003.  
<https://doi.org/10.5194/ms-12-997-2021>
- [30] H. Dong, Y. Bi, Z.-B. Liu, X.-L. Zhao, Establishment and analysis of nonlinear frequency response model of planetary gear transmission system. *Mechanical Sciences*, 12(2), 2012: 1093-1104.  
<https://doi.org/10.5194/ms-12-1093-2021>